Bio-optical properties of the Labrador Sea

Glenn F. Cota,[1] W. Glen Harrison,[2] Trevor Platt,[2] Shubha Sathyendranath,[3] and Venetia Stuart[2]

Received 21 August 2000; revised 11 March 2003; accepted 11 April 2003; published 15 July 2003.

[1] Three cruises were conducted during fall and spring in the Labrador Sea to investigate the effects of bio-optical properties on satellite retrievals of phytoplankton chlorophyll in this important high-latitude ecosystem. Taxon-specific and regional differences were found. Diatoms had ~1.5 lower chlorophyll-specific absorption but significantly higher reflectance ratios than prymnesiophytes. Particulate absorption at 443 nm for total, phytoplankton, and "detrital" fractions was related to chlorophyll, but values were lower than reported for lower latitudes. Decreased particulate absorption is attributed primarily to pigment packaging, while low backscattering to scattering ratios result from a lower relative abundance of bacteria and picophytoplankton with more large phytoplankton. Soluble absorption was not related to chlorophyll. A four-component model with low, variable backscatter fractions and the observed absorption coefficients for phytoplankton, "detritus," and soluble materials reproduces the measured reflectance spectra. Global chlorophyll algorithms tend to underestimate biomass at high latitudes, whereas regionally tuned algorithms provide more reliable retrievals. Taxon-specific algorithms show promise, but given limited ranges, small sample sizes, and overlapping reflectance ratios they remain premature. *INDEX TERMS:* 4552 Oceanography: Physical: Ocean optics; 4855 Oceanography: Biological and Chemical: Plankton; 9315 Information Related to Geographic Region: Arctic region; 4275 Oceanography: General: Remote sensing and electromagnetic processes (0689); *KEYWORDS:* Labrador Sea, bio-optics, ocean color, remote sensing, chlorophyll, phytoplankton

Citation: Cota, G. F., W. G. Harrison, T. Platt, S. Sathyendranath, and V. Stuart, Bio-optical properties of the Labrador Sea, *J. Geophys. Res.*, *108*(C7), 3228, doi:10.1029/2000JC000597, 2003.

1. Introduction

[2] Satellites have provided unprecedented views of features and processes across many scales in the global oceans. The potential utility of ocean color observations was established with the Coastal Zone Color Scanner (CZCS) program, which emphasized the need for more comprehensive approaches of evaluating algorithm performance to gain a better understanding of the ocean's role in biogeochemical cycles. CZCS imagery indicated that many high-latitude regions are among the most productive (i.e., large biomass accumulations) in the world [*McClain et al.*, 1993], but there were numerous interpretational problems and very little field data to confirm the results [e.g., *Müller-Karger et al.*, 1990]. Cloud and ice cover limit useful imagery, but CZCS frequently did not collect data at high latitudes. Seasonal climatologies for most high-latitude regions were based on <400 images over the 8 years CZCS operated [*McClain et al.*, 1993]. Most importantly, there were no contemporaneous optical validation data collected in the atmosphere or ocean at high latitude to improve atmospheric corrections and chlorophyll retrievals. The few post-CZCS studies of in-water bio-optics for high-latitude marine ecosystems were summarized by *Mitchell* [1992].

[3] Oceanographic surveys and satellite observations both indicate that the Labrador Sea is a productive region. *Steemann Nielsen* [1958] reported elevated rates of production near frontal boundaries and in Greenland coastal waters. Seasonal composites of CZCS imagery suggest that coastal waters are very productive [*McClain et al.*, 1993], but mask transient mesoscale features and water mass discontinuities. Phytoplankton and optical data for this region have very limited spatial and temporal coverage. Many details of phytoplankton dynamics remain to be quantified, but seasonal trends and patterns are emerging from the Sea-viewing Wide-Field-of-view Sensor (SeaWiFS). Monthly SeaWiFS climatologies (http://seawifs.gsfc.nasa.gov) for 1998–2002 reveal similar seasonal dynamics. The phytoplankton bloom in the Labrador Sea commences in April primarily in the northeastern sector; there is also elevated biomass along the ice edge to the north and west and in coastal waters out to slope regions. Almost the eastern third of the Labrador Sea is in full bloom by May, as well as blooms along retreating ice edges in the northern and western regions. In June the central basin has relatively low chlorophyll concentrations and elevated biomass is most pronounced over shelves particularly off southern

[1]Center for Coastal Physical Oceanography, Old Dominion University, Norfolk, Virginia, USA.
[2]Biological Oceanography, Bedford Institute of Oceanography, Dartmouth, Nova Scotia, Canada.
[3]Department of Oceanography, Dalhousie University, Halifax, Nova Scotia, Canada.

0148-0227/03/2000JC000597

Labrador. Moderate biomass occurs over much of the deep basin from July through September or even early October. Most shelf regions remain lower than the basin except east-southeast of the Hudson Strait, which may reflect the outflow. There appears to be a fall bloom over shelf and slope regions in September on the Greenland side and in October on the Labrador side. In general, this region displays elevated chlorophyll biomass in various sectors over most of the growing season from April through September or October. However, while these patterns may be robust, operational global algorithms often do not provide accurate chlorophyll retrievals regionally as shown below.

[4] Our primary objectives were to: (1) investigate the bio-optical properties of the soluble and particulate materials and (2) develop bio-optical algorithms for determining phytoplankton biomass at high northern latitudes with ocean color satellites such as the Ocean Color and Temperature Sensor (OCTS), SeaWiFS, the MODerate-resolution Imaging Spectrometer (MODIS), and the Global Imager (GLI). Large in situ data sets, spanning a broad range of environmental conditions, are necessary to develop and evaluate algorithm performance in any given region, let alone globally. Operational algorithms for OCTS and SeaWiFS are compared with our regionally tuned algorithms. Absorption properties of all major optically active components were collected to better understand potential differences within this ecosystem and between taxa. Our bio-optical observations are compared with those from other regions, and Hydrolight simulations [*Mobley*, 1994, also personal communication] were used to corroborate observations and gain further insight into their variability. Improved chlorophyll retrievals will help elucidate the role of phytoplankton in biogeochemical cycles at high latitudes, since operational algorithms tend to underestimate high-latitude blooms [e.g., *Mitchell*, 1992, this study].

2. Methods

[5] Bio-optical validation observations were made on the CCGS Hudson in fall from 16 October to 17 November 1996, in spring from 9 May to 11 June 1997, and again from 22 May to 7 June 2000 in the Labrador Sea. Stations were occupied along several sections between Labrador and Greenland (Figure 1) with some locations revisited more than once during a cruise. The most heavily sampled SW-NE section in Figure 1 from Hamilton Bank on the Labrador Shelf to Cape Desolation on the Greenland Shelf is the AR7 line of the World Ocean Circulation Experiment. The first two cruises coincided closely with the beginning and end of the observational period for Japan's OCTS and represent the first ocean color validation data for this region.

2.1. Discrete Measurements

[6] Discrete water samples for biogeochemical observations were collected with Niskin bottles or a pump at 10 m intervals from near surface to a depth of 100 m. Particulate materials were collected on Whatman® GF/F glass fiber filters, while soluble materials were the filtrate from Gelman® 0.2 μm membrane filters. Chlorophyll and phaeopigments were determined fluorometerically [*Parsons et al.*, 1984] in 90% acetone after ~24 hour extraction at −20°C.

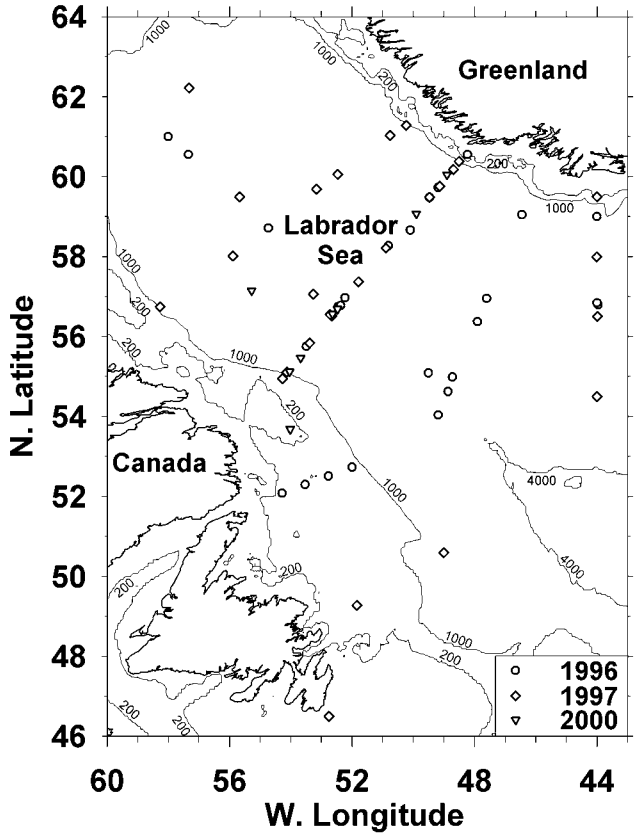

Figure 1. Labrador Sea with bio-optical stations for cruises in fall 1996 (circles), spring 1997 (diamonds), and spring 2000 (inverted triangles).

Pigment composition was determined on a select subset of samples, which were stored at −70°C until analyzed with reverse-phase, high-performance liquid chromatography (HPLC) [*Head and Horne*, 1993]. Frozen HPLC filters were homogenized in 1.5 ml 90% acetone, centrifuged, and diluted with 0.5 *M* aqueous ammonium acetate at a ratio of 1:2 before injection. Peak identifications were made using standards for chl-*a*, -*b*, and -*c* (mixture of c_1 and c_2), fucoxanthin, β-carotene, 19-butanoyloyxfucoxanthin, 19-hexanoyloxyfucoxanthin, diadinoxanthin, lutein, and zeaxanthin. Standards of chl-*a*, chl-*b*, and β-carotene were obtained from Sigma Chemical Co., and other standards were provided by R. Bidigare.

[7] Absorption spectra were determined on total particulate $a_p(\lambda)$ [*Mitchell*, 1990], nonpigmented particulates $a_n(\lambda)$ extracted with unheated 100% methanol [*Kishino et al.*, 1985], and filter-passing soluble $a_s(\lambda)$ materials [*Bricaud et al.*, 1981]. These classes are operationally defined. The particulate fractions are mixtures including phytoplankton, bacteria, protozoans, multicellular microheterotrophs, and nonliving organic and inorganic particles. The residual particles after methanol extraction are not simply equivalent to a "detrital" fraction. Algal or phytoplankton absorption $a_a(\lambda)$ was estimated as the difference between $a_p(\lambda)$ and $a_n(\lambda)$; this approach implicitly assumes that algal cells contain the vast majority of photosynthetic and nonphotosynthetic pigments. Absorption by algal cells a_a has been variously designated as a_{ph} (phytoplankton) or a_ϕ, non-

pigmented particles a_n as a_d (detritus) or a_{det} (detritus) or a_{nap} (nonalgal particles), and soluble materials a_s as a_y (yellow matter) and a_d (dissolved). These designations are, more or less, interchangeable depending upon the techniques employed. Absorption coefficients were normalized to fluorometric chlorophyll.

2.2. Continuous Vertical Profiles

[8] In-water optical measurements were made with a Satlantic free-fall profiling spectral radiometer and a subsurface reference. The instrument had 13 channels for downwelling spectral irradiance $E_d(\lambda)$ and upwelling radiance $L_u(\lambda)$ on the profiler and reference with nominal central wavelengths of 405, 412, 443, 490, 510, 520, 532, 555, 565, 620, 665, 683, and 700 nm. It had tilt and roll sensors, a pressure sensor, and a conductivity-temperature sensor. The radiometers were deployed with Kevlar conducting cables and acquired data at 6 Hz. A black surface float (2 m^2) suspended the surface incident spectral irradiance (E_{s0-}) sensors 0.3 m below the surface, while the radiance ($L_{u1.5-}$) head was about 1.2 m. The profiler sank at about 0.8–1.0 m s^{-1}, so six to eight measurements per meter of $E_d(\lambda,z)$ and $L_u(\lambda,z)$ were obtained. Optical casts were normally done over the top 70–100 m within 3 hours of local solar noon. Ship shadow was minimized with all radiometric sensors >20 m away from the ship toward the Sun. Only one station was removed because of ship shadow effects.

[9] Optical data acquisition and analyses were in accord with the latest SeaWiFS protocols [*Mueller and Austin*, 1995]. Optical data were processed with Satlantic's ProSoft software version 6.3d (ftp://ftp.satlantic.com/pub/optics/dalhousie). Data from each cast were edited by removing the top or bottom of profiles with excessive tilt (>5°), corrected for recent instrument calibration, and then binned at 1 m intervals. Vertical attenuation coefficients were estimated over 11–15 m intervals to reduce wave-focusing effects. Radiance profiles were extrapolated to and through the air-water interface correcting for attenuation, reflection, and refraction to estimate water-leaving radiance $L_w(\lambda,0^+)$, which was also normalized to incident radiation at the top of the atmosphere to obtain normalized water-leaving radiance $L_{\mathrm{wn}}(\lambda)$. Remote sensing reflectance $R_{\mathrm{rs}}(\lambda)$ was computed as the ratio of $L_u(\lambda,0^+)$ divided by incident irradiance $E_s(\lambda,0^+)$ just above the surface. Ratios of remote sensing reflectance or normalized water leaving radiance from two to four channels were regressed against surface (fluorometric) chlorophyll concentrations to establish bio-optical algorithms for phytoplankton biomass retrieval [*Kishino et al.*, 1998; *O'Reilly et al.*, 1998, 2000]. All algorithms were derived from $\log_{10}$ transformed data. Over 320 linear and nonlinear candidate equations were fitted to various wavelength combinations with Table Curve 2D (Jandel Scientific) software to evaluate algorithms. Model II linear regression analyses were employed because both variables were measured with error [*Sokal and Rohlf*, 1995].

2.3. Bio-Optical Modeling

[10] Bio-optical simulations of the Labrador Sea were conducted with HydroLight 4.1 [*Mobley*, 1994, also personal communication] with a four-component model including pure water, phytoplankton, nonpigmented particles, and colored dissolved organic materials (CDOM). Concentrations of chlorophyll, CDOM, and nonpigmented particles were held constant over the top 20 m (i.e., a surface mixed layer) with an infinitely deep bottom boundary. Multiwavelength runs from 350 to 700 nm were done for solar noon on 1 June at a central location (56.55°N, 52.71°W), with cloud-free skies, a wind speed of 5 m s^{-1}, and a semiempirical sky model. Runs for 1 November differed by a maximum of 5–7% over the blue-green for the lowest biomass level and diminish to 1–3% for high biomass. Solar forcing for direct and diffuse downwelling irradiance is obtained from the RADTRAN model [*Gregg and Carder*, 1990] with normalized angular patterns of sky radiance [*Mobley*, 1994, also personal communication].

[11] The inherent optical property (IOP) specifications in the model runs relied on observed values or the literature. Water absorption and scattering were based on the work of *Pope and Fry* [1997] and *Smith and Baker* [1981], respectively. Specific-absorption spectra from 350 to 700 nm for phytoplankton and nonpigmented particles were based on observed coefficients normalized to chlorophyll concentration. The average chlorophyll-specific CDOM spectrum was held constant because it varied little with biomass (see below). Scattering for chlorophyll-containing and nonpigmented particles was specified by:

$$b_p(\lambda) = 0.2C^{0.6}(550/\lambda)^3, \tag{1}$$

where λ is wavelength in nm, 550 is the reference wavelength, and C is chlorophyll concentration (mg m^{-3}). This relationship increases the spectral dependency of scattering (m = 3) compared with *Gordon and Morel*'s [1983] or *Loisel and Morel*'s [1998] equations (m = 1) and represents the only model customization utilized to simulate these data. Inelastic scattering was included for Raman, chlorophyll fluorescence, and CDOM fluorescence; bioluminescence was not. Fournier-Forand phase functions were selected with backscattering to scattering (b_b/b) fractions proportional to chlorophyll concentrations as outlined by *Ulloa et al.* [1994].

3. Results and Discussion

3.1. Oceanographic Conditions

[12] Oceanographic conditions throughout most of the study area in October–November 1996 were characterized by relatively deep surface mixed layers, which were often in excess of 60–80 m. Euphotic zone depths (i.e., 1% of incident irradiance) ranged from 24 to 76 m with a mean ± standard deviation of 52 ± 13 m for 74 optical profiles. Chlorophyll concentrations at these stations were relatively low, averaging 1.2 ± 1.6 mg m^{-3} at the surface and 47 ± 38 mg m^{-2} integrated over the euphotic zone. Late spring conditions in May–June 1997 and 2000 displayed more vertical structure with shallower mixed layers, particularly shoreward of slope regions, and higher phytoplankton biomass. In 1997 euphotic depths ranged from 15 to 49 m with a mean of 31 ± 9 m for 76 profiles. Chlorophyll concentrations near surface ranged from 0.52 to 13.3 mg m^{-3} and averaged 2.2 ± 2.7 mg m^{-3}. Integrated chlorophyll concentrations in spring 1997 ranged from 40 to 197 mg m^{-2} with a mean of 99 ± 55 mg m^{-2}. Euphotic depths were slightly deeper in 2000 with an average of 44 ± 13 m for 24 profiles (range

16–63 m). Surface chlorophyll concentrations ranged from 0.60 to 9.6 mg m^{-3} and averaged 2.2 ± 2.7 mg m^{-3} in 2000, while integrated euphotic zone values had a mean of 67 ± 49 mg m^{-2} with a range of 23–179 mg m^{-2}.

[13] Surface chlorophyll concentrations were very closely related to both mean euphotic layer chlorophyll (r^2 = 0.97) and vertically integrated chlorophyll (r^2 = 0.94) concentrations in the euphotic zone for the log-transformed values. Hence volumetric and areal values are well represented by surface concentrations even if vertical structure is not available.

[14] The optical stations collected during fall 1996, spring 1997, and spring 2000 (Figure 1) represent a small subset of the oceanographic observations for these multidisciplinary cruises. The bio-optical data sets span chlorophyll concentrations from about 0.05 to >13 mg m^{-3} and encompassed much of the natural range for this region. However, other related data sets aid in the interpretation of regional features and dynamics.

[15] Chlorophyll distributions illustrate that the Labrador Sea is a highly productive region. Considerable biomass was found at subeuphotic depths and high concentrations were noted at a number of stations with and without optical measurements. In 1997 integrated chlorophyll in the upper 100 m was >300 mg m^{-2} at seven stations in Greenland shelf and slope waters with >1000 mg m^{-2} at two of those stations. Several stations with >300 mg chlorophyll m^{-2} were also occupied in deep waters of the central basin in late May and in Newfoundland shelf waters in early June 1997. By contrast, only one station with >300 mg chlorophyll m^{-2} was encountered in spring 2000 and late October 1996 in deep water off the slope of Greenland. Between 17 and 64% of the profile stations on each cruise had >100 mg chlorophyll m^{-2} in the upper 100 m, so phytoplankton biomass was frequently >1 mg chlorophyll m^{-3} even in fall.

3.2. Phytoplankton Assemblages

[16] Pigment composition data were collected at select stations and depths, typically one near surface and another lower in the euphotic zone within the chlorophyll maximum (V. Stuart, unpublished data, 1996, 1997, 2000). Phytoplankton assemblages were distinguished by a dominant group when pigment composition was available or were designated as "unidentified" (U) in their absence. Those dominated by diatoms (D) and prymnesiophytes (P, n.b. prymnesiophytes are a typified division name for haptophytes) had chlorophyll *c*3 to chlorophyll *a* ratios below and above 0.025, respectively, similar to the demarcation schemes of *Stuart et al.* [2000] and *Sathyendranath et al.* [2001] for this region. With deep mixing in fall, prymnesiophytes dominated pigment signatures at all but 2 out of 18 stations. Diatoms dominated 11 of 27 stations examined in spring 1997 and were dominant only near surface at 2 of the 11 stations. During spring 2000 fewer stations were occupied, but nutrient concentrations displayed little drawdown in most cases, suggesting an earlier phase of the growth season in 2000 compared with 1997 (W. G. Harrison, unpublished data, 1996, 1997, 2000). Diatoms dominated 6 of 20 surface intake samples in spring 2000, but only 1 of 9 stations with vertical sampling. In 2000 almost a third of surface and subsurface samples exhibited chlorophyll *c*3 to chlorophyll *a* ratios between 0.028 and 0.035, so the distinction between groups was less clear and may have represented a transitional phase in species succession.

[17] Pigment ratios were variable, but seemed to be indicative of the predominant taxonomic groups (Table 1). Diatom and prymnesiophyte-dominated assemblages had significantly different pigment ratios as shown in Table 1 [two-tailed *t*-test with unequal variance, $P < 0.001$, *Sokal and Rohlf*, 1995]. Chl-*a* estimated by HPLC was ~71% of that estimated fluorometrically and there was no systematic difference between the phytoplankton groups. Chl-*b*, typically attributed to chlorophytes, was detectable in all but 11 samples. Chl-*b*/*a* ratios were highly variable but significantly different ($P < 0.01$) with prymnesiophyte- and diatom-dominated samples averaging 0.12 ± 0.07 and 0.07 ± 0.07, respectively. Chl-*b* can decrease fluorometric estimates of chl-*a* and increase apparent phaeopigment concentrations [see *Parsons et al.*, 1984 and references cited therein].

[18] The use of pigments in natural samples to identify major taxonomic groups has become fairly common, but is rarely unequivocal. This is particularly true in the absence of clear, corroborating evidence such as cell counts and size fractionations [*Bidigare et al.*, 1996; *Stuart et al.*, 2000] or obvious patterns of nutrient depletion [e.g., *Smith et al.*, 1991]. Natural assemblages are complex mixtures with many species from a variety of taxa, which occur in many combinations. High-latitude blooms tend to be dominated by either diatoms or prymnesiophytes and often have one or a few dominant species in blooms. However, pigment complements and ratios for diatoms and prymnesiophytes in culture can be highly variable [*Stauber and Jeffrey*, 1988; *Jeffrey and Wright*, 1994]. There can be considerable overlap in pigment composition, i.e., *Jeffrey and Wright*'s [1994] haptophyte types 1 and 2 are both similar to diatoms. Polar species are nearly absent in culture surveys, and extensive evaluations of the response of pigment composition in polar species to environmental variation are lacking. According to *Jeffrey and Wright* [1994], "No clear-cut pigment pattern for all haptophytes has emerged, which emphasizes the caution oceanographers must still exercise in identification of this group of planktonic algae from pigment signatures." Given a continuum of mixtures in seasonal succession, environmental variability, and acclimation status, care should be taken to avoid overinterpretation of taxonomic "dominance" in natural assemblages based solely on pigment composition.

3.3. Absorption Characteristics of Particulate and Soluble Materials

[19] The optical properties of case 1 waters are nominally determined by the variability of phytoplankton chlorophyll and its degradation products. Apparent optical properties (AOPs) such as remote sensing reflectance (R_{rs}) and normalized water-leaving radiance (L_{wn}) are the measured quantities of interest in remote sensing applications, but the AOPs depend upon the absorption and scattering or IOPs of a water body. The absorption characteristics of optically active constituents from our cruises help explain differences between the bio-optical properties of these high-latitude waters versus more widely studied lower latitude ecosystems.

3.3.1. Absorption Spectra

[20] Spectral absorption coefficients were determined for total particulates, nonpigmented particulates, and soluble

Table 1. Pigment Composition in the Labrador Sea[a]

Group	All	Diatoms	Prymnesiophytes
Observations	125	29	96
chl *c*3:chl *a*	0.042 ± 0.022	0.014 ± 0.008	0.051 ± 0.017
fuco:chl *a*	0.313 ± 0.145	0.427 ± 0.128	0.278 ± 0.131
hex:chl *a*	0.152 ± 0.100	0.049 ± 0.050	0.182 ± 0.090
allo:chl *a*	0.012 ± 0.018	0.005 ± 0.010	0.014 ± 0.019
H:F	0.710 ± 0.200	0.726 ± 0.267	0.705 ± 0.176

[a]Pigments include chlorophyll *a* (chl *a*), chlorophyll *c*3 (chl *c*3), fucoxanthin (fuco), 19′hexanolyoxyfucoxanthin (hex), and alloxanthin (allo). The ratio for paired samples of chlorophyll *a* estimated by HPLC to fluorometry (H:F) are also presented.

materials within the euphotic zone of optical stations (Figure 2). Phytoplankton or algal absorption spectra (Figure 2c) were estimated as the difference between sequential measurements of total and nonpigmented particles extracted with methanol. The mean ± one standard deviation is presented for each absorption spectra in Figure 2. The dominant influence of phytoplankton on the total particulate absorption spectrum (Figure 2a) is evident from the chlorophyll absorption peaks around 440 and 675 nm. The presence of nonpigmented particles (Figure 2b) and accessory pigments masks the blue peak partially, while the phytoplankton absorption spectrum shows the blue and red peaks more clearly (Figure 2c). Prymnesiophyte absorption coefficients were ~1.5 times higher than diatom (Figure 3a) in the blue and mean spectra for either taxonomic group were outside one standard deviation of the other group. This difference is consistent with more highly packaged pigments in larger diatom cells. Prymnesiophytes had a more pronounced shouldering at ~475 nm, which may be due to elevated levels of alloxanthin and 19′-hexanoyloxyfucoxanthin (Table 1). When both spectra are normalized to unity at 675 nm (Figure 3b) discrepancies between the groups are more obvious, especially in the resulting difference spectrum (inset Figure 3b). Prymnesiophytes are more adept at harvesting blue-green light and thus should have a competitive advantage in deeper mixed layers [*Cota et al.*, 1994].

[21] Phytoplankton absorption depends on many factors including pigment composition, concentration, and packaging, light history, cell size, etc., but regional comparisons are of interest. Our high-latitude coefficients fall within the range reported by *Bricaud et al.* [1998] for a large data set (n = 1166) normalized to chlorophyll from a number of lower latitude cruises. For total particulates and phytoplankton the magnitudes of the red and blue absorption peaks have been reported in only a few previous high-latitude studies and unfortunately many of these were normalized to chlorophyll plus phaeopigments (Table 2). Comparisons

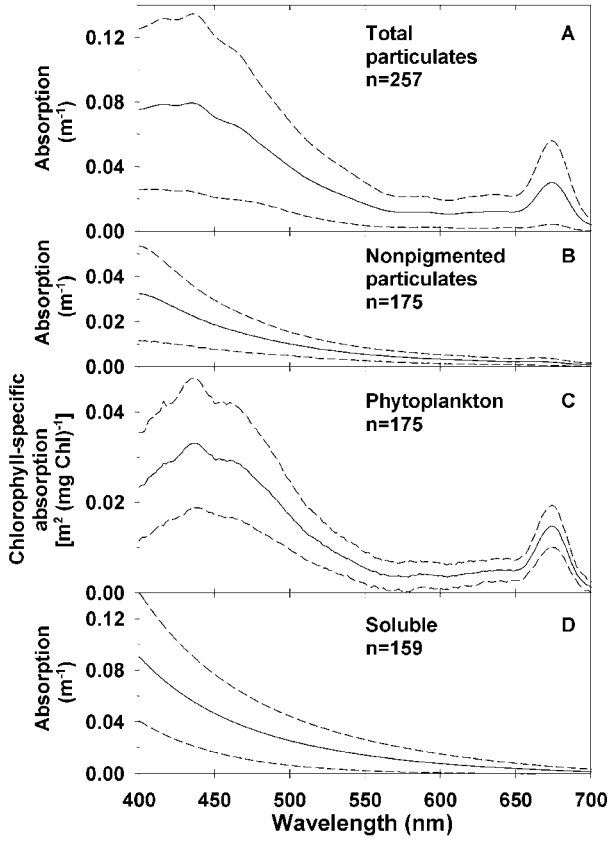

Figure 2. Mean absorption spectra (solid lines) for (a) total and (b) nonpigmented particulates, (c) chlorophyll-specific absorption, and (d) soluble materials for phytoplankton plus/minus one standard deviation (dotted lines). n, number of observations.

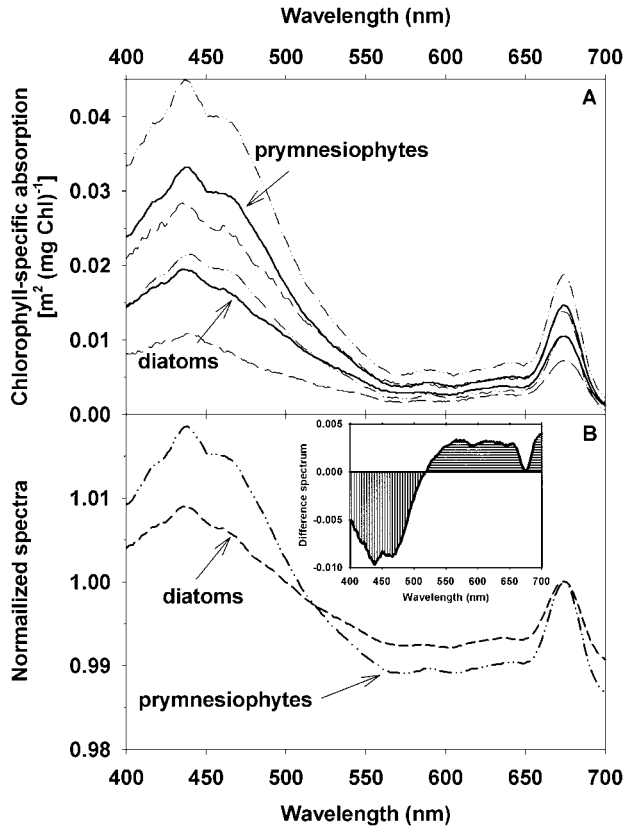

Figure 3. (a) Mean absorption spectra (solid lines) plus/minus one standard deviation for prymnesiophytes (dash-dotted lines) and diatoms (dashed lines). (b) Mean spectra for each taxon normalized to unity at 675 nm, where the inset shows their difference spectrum.

Table 2. Specific Absorption in the Blue (435–443 nm) and Red (670–676 nm) Peaks for Total Particulates a_p^* or Phytoplankton a_a^* (m^2 (mg pigment^{-1})) for Various Regions[a]

Location	Source	Type	Pigment	[Chl]	Blue Peak	Red Peak	443/555	490/555
				Total Particulate Absorption: a_p^*				
Bransfield Strait	1	all	CP	NR	0.018 (0.015–0.035)	NR		
Greenland Sea	2	P	CP	NR	0.040	NR		
Gerlache Strait	3	Cr	CP	NR	0.046	NR		
Gerlache Strait	3	D	CP	NR	0.017	NR		
Greenland Sea	4	P	CP	0.11–7.21	0.056 ± 0.072	0.023 ± 0.011		
Resolute	7	all	C	0.08–36.1	0.020 ± 0.022	0.009 ± 0.010		
Labrador Sea	8	all	C	0.08–13.2	0.043 ± 0.020	0.014 ± 0.005		
Lower latitudes	9	all	C	0.02–25	~0.003 to 0.145	NR		
				Phytoplankton Absorption: a_a^*				
Ross Sea	5	all	CP	NR	0.041 ± 0.015	0.023 ± NR		
Ross Sea	5	D	CP	NR	NR	NR	6.24 ± 2.11	4.03 ± 1.19
Ross Sea	5	P	CP	NR	NR	NR	8.03 ± 3.10	5.26 ± 1.93
Ross Sea	5	Cr	CP	NR	NR	NR	4.13 ± 3.10	2.54 ± 0.36
Labrador Sea	6	D	C	0.14–11.7	0.015 ± 0.006[b]	0.008 ± 0.002b	3.73 ± 0.75	2.44 ± 0.63
Labrador Sea	6	P	C	0.17–9.33	0.037 ± 0.008b	0.017 ± 0.002b	6.30 ± 0.91	4.27 ± 0.52
Resolute	7	all	C	0.08–36.1	0.010 ± 0.004	0.006 ± 0.002	4.20 ± 0.75	2.46 ± 0.35
Labrador Sea	8	all	C	0.08–13.2	0.032 ± 0.014	0.014 ± 0.004	6.27 ± 2.75	4.02 ± 1.78
Labrador Sea	8	D	C	0.36–9.68	0.019 ± 0.008	0.010 ± 0.003	5.25 ± 1.98	3.55 ± 1.20
Labrador Sea	8	P	C	0.32–13.2	0.032 ± 0.011	0.014 ± 0.004	6.35 ± 1.50	4.83 ± 1.10
Lower latitudes	9	all	C	0.02–25	~0.0015 to 0.130			

[a]Pigment refers to chlorophyll (C) or chlorophyll plus phaeopigments (CP). Values are means ± standard deviations or ranges. Sources include: (1) *Mitchell and Holm-Hansen* [1991], (2) *Mitchell* [1992], (3) *Brody et al.* [1992], (4) *Cota et al.* [1994], (5) *Arrigo et al.* [1998], (6) *Stuart et al.* [2000, also unpublished data], (7) Cota (unpublished data), (8) this study, (9) and *Bricaud et al.* [1998]. Algal types include: Cryptomonads (Cr), Diatoms (D), Prymnesiophytes (P); all types or unidentified mixtures (all). NR is not reported. Chl is chlorophyll concentration range in mg m^{-3}.
[b]Normalized to fluorometric chlorophyll not HPLC chlorophyll as published.

between absorption spectra are more straightforward in the red where there is less potential interference by accessory pigments and other materials. The most striking difference in Table 2 is that the pigment-specific red-peak absorption of *Arrigo et al.* [1998] at 676 nm for phytoplankton is about 2–4 times higher than all other studies except the prymnesiophyte assemblage of *Stuart et al.* [2000]. The discrepancy would have been even larger if they had normalized to chlorophyll instead of pigment (chlorophyll plus phaeopigments) or used *Mitchell's* [1990] beta algorithm for path length amplification correction. *Arrigo et al.* [1998] also suggest that their absorption data reflect the fact that "light levels were unusually high before and during" their cruise. Incident photosynthetically active radiation (PAR, 400–700 nm) just below the sea surface (E_{s0-}) averaged 460 ± 362 μmol photons m^{-2} s^{-1} in their study. In the Labrador Sea comparable E_{s0-} values were only 169 ± 117 μmol photons m^{-2} s^{-1} in fall 1996 (n = 77), but 786 ± 456 μmol photons m^{-2} s^{-1} in spring 1997 (n = 83), and 815 ± 418 μmol photons m^{-2} s^{-1} in spring 2000 (n = 24). In Resolute Passage (~74.36°N) mean E_{s0-} values for PAR were 367 ± 171 (n = 27), 461 ± 209 (n = 52), 521 ± 212 (n = 33), and 593 ± 242 (n = 91) μmol photons m^{-2} s^{-1} during four field programs in August from 1994 to 1998; values can exceed 900 μmol photons m^{-2} s^{-1} at solar noon on clear days (G. F. Cota, unpublished data, 1994–1996, 1998). Hence the Ross Sea observations by *Arrigo et al.* [1998] do not seem to be particularly bright compared with other high-latitude ecosystems.

[22] Cell size may help explain the differences observed between the absorption values found in the studies listed in Table 2. *Arrigo et al.* [1998] reported volumes for small cells with equivalent spherical diameters of about 4.7, 6.6, and 12.5 μm, respectively, for diatoms, *Phaeocystis antarctica*, and cryptophytes. By contrast, *Brody et al.* [1992] found large diatoms (≥20 μm diameter) and small cryptophytes (≤5 μm diameter). In the high Canadian Arctic, we (G. F. Cota, unpublished data, XXXX) observed mean diameters of ≥20 and ~3 μm for the predominant diatoms and flagellates, respectively. In size-fractionated samples, *Stuart et al.* [2000] found that >96% of chlorophyll was >3 μm for diatom-dominated stations, whereas 40–80% of chlorophyll was <3 μm at prymnesiophyte-dominated stations; pump collections apparently disrupted *Phaeocystis* colonies but not cellular integrity and had little effect on chlorophyll concentrations or particulate absorption (see Appendix 1 of *Stuart et al.* [2000]).

[23] Larger cells tend to have more highly packaged pigments [see *Kirk*, 1994 and references cited therein]. However, size determinations of cells are not always comparable nor even particularly reliable for various techniques or particular taxonomic groups. Most measurement techniques and models also reduce cells to spherical equivalents, which can mask important morphological differences and colonial structures. Microscopic measurements of "preserved" diatoms or other forms with more rigid cell wall materials can be highly accurate, but cell deformation (e.g., shrinkage) of unarmored flagellate cells can compromise measurements. Microscopic measurements are often based on a relatively small sample size too. Particle counters typically count many unpreserved cells and nonliving materials, particularly smaller more abundant particles. More sophisticated counting systems, such as flow cytometers, distinguish debris and cells based on fluorescence properties. It is impossible to fully evaluate the discrepancies in spectral absorption characteristics without more information about the data and details on counting methods used in the studies in Table 2. The values reported by *Arrigo*

et al. [1998] and *Stuart et al.* [2000] represent single cruises, yet the former are even more variable than three different cruises from two seasons in this study (Table 2).

[24] Ocean color algorithms typically utilize blue and green wave bands from about 440 to 565 nm and sufficiently large taxon-specific differences in absorption within this spectral region may influence chlorophyll retrievals. Diatoms displayed significantly lower ratios for chlorophyll-specific absorption at 443/555 and 490/555 nm compared with prymnesiophytes (Table 2). Similar trends have been observed in the Labrador Sea [*Stuart et al.*, 2000] and in the Ross Sea by *Arrigo et al.* [1998]; the later study reported considerably higher ratios for both taxonomic groups at those wave bands. Differences in bio-optical signatures help distinguish various taxa, but the magnitudes may not be sufficiently large to clearly demarcate one taxon from the other given the observed regional and seasonal variability. During seasonal succession when species mixtures are nearly equal, particular taxa may not be readily distinguished. However, during blooms, where one or a few species from a single taxon dominates, bio-optical signatures may indeed be clearly different. Because high-latitude ecosystems are characterized by strongly pulsed production with dominance by either diatoms or prymnesiophytes in blooms [e.g., *Smith et al.*, 1991; *Stuart et al.*, 2000], the utility of taxon-specific bio-optical relationships may be greater than at lower latitudes.

[25] Absorption by colored constituents other than phytoplankton accounts for a large portion of total nonwater absorption. Based on the mean observed spectra (Figure 2), soluble absorption accounts for 38–47% of total nonwater absorption for particulate plus soluble materials in blue and green channels from 443 to 555 nm. The large contribution by soluble materials may have a significant impact on chlorophyll retrievals [e.g., *Carder et al.*, 1989; *Sathyendranath et al.*, 2001], and as described below, it does not covary closely with chlorophyll.

3.3.2. Relationships Between Phytoplankton Biomass and Absorption

[26] Variability of optically active constituents in case 1 waters is often related to chlorophyll concentration. Relationships between particulate ($a_{p(443)}$) or algal ($a_{a(443)}$) absorption coefficients at 443 nm and chlorophyll concentration are typically nonlinear, and power functions provide reasonable approximations [e.g., *Bricaud et al.*, 1995, 1998]. Figure 4 shows power functions for absorption coefficients at 443 nm for each constituent versus chlorophyll concentration [Chl]:

$$a_{p(443)} = 0.0542[\mathrm{Chl}]^{0.544}, \quad r^2 = 0.80, \quad n = 257, \qquad (2)$$

$$a_{a(443)} = 0.0402[\mathrm{Chl}]^{0.578}, \quad r^2 = 0.73, \quad n = 175, \qquad (3)$$

$$a_{n(443)} = 0.0151[\mathrm{Chl}]^{0.410}, \quad r^2 = 0.55, \quad n = 175, \qquad (4)$$

$$a_{s(443)} = 0.0502[\mathrm{Chl}]^{0.086}, \quad r^2 = 0.02, \quad n = 159, \qquad (5)$$

where r^2 is the coefficient of determination and n is the number of observations. Our relatively small regional data sets show fairly strong relationships between total particulate absorption or phytoplankton absorption and chlorophyll explaining 80 and 73% of their variability. *Bricaud et al.* [1998] noted determination coefficients of 0.90 and 0.91, respectively, for total particulate and algal fractions with a much larger and diverse observational database (n = 1166). However, *Bricaud et al.* [1995] reported determination coefficients of only 0.49 (n = 327 without LIDAR data sets) and 0.77 for their combined data sets (n = 815) for blue peak absorption ($a_{a(440)}$) by phytoplankton as a function of chlorophyll concentration. Even though more restricted, our Labrador Sea data fall within the 90% confidence limits of *Bricaud et al.* [1998], which were proposed as realistic upper and lower bounds. Their coefficients for total and phytoplankton components fall within the 95% confidence limits of ours, but our exponent for total particulate matter (i.e., 0.544 with a 95% confidence interval from 0.508 to 0.580) is significantly lower. We would predict 13% more and 15% less absorption by total particulates at biomass levels of 0.3 and 10 mg chlorophyll m^{-3}, respectively. This discrepancy may be due, in part, to our unequal sample sizes with $a_{p(443)}$ containing more low fall values versus a higher frequency of higher biomass $a_{a(443)}$ samples from spring.

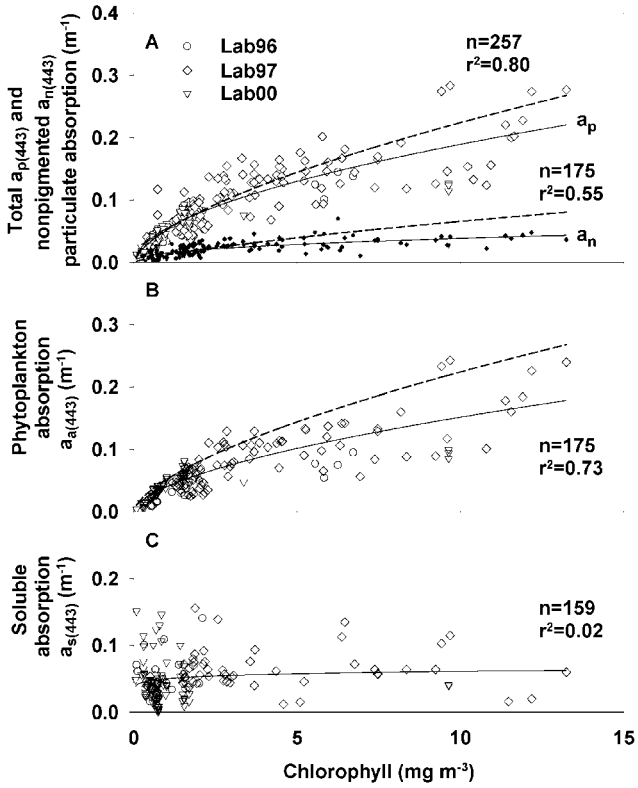

Figure 4. Power functions for (a) total and nonpigmented particulate, (b) phytoplankton, (c) and soluble absorption at 443 nm versus chlorophyll concentration. Samples sizes (n), coefficients of determination (r^2), and years of collection are shown for 1996 (circles), 1997 (diamonds), and 2000 (inverted triangles) data. Smaller solid symbols refer to nonpigmented particulates for each year (Figure 4a). Dashed lines in Figures 4a and 4b are from *Bricaud et al.* [1998].

[27] Absorption at 443 nm by nonpigmented particulate materials versus chlorophyll follows a different trend at higher latitude (Figure 4a). *Bricaud et al.* [1998] found that phytoplankton and nonpigmented materials were a relatively constant portion of total particulates at about 73% (71–75%) and ~24% (17–32%), respectively, over chlorophyll concentrations from 0.02 to 25 mg m^{-3}. Our relationship for $a_{n(443)}$ predicts higher absorption by nonpigmented particles at low biomass levels (>40% of $a_{p(443)}$ at 0.3 mg chlorophyll m) and lower absorption (<20% of $a_{p(443)}$) for chlorophyll concentrations over 10 mg m^{-3}. Figure 5a shows that the contribution to total particulate absorption by nonpigmented particles is highly variable, especially at low biomass. Phytoplankton absorption accounted for around 35–65 and 75–85%, respectively, at low and high biomass (Figure 4b). For a given chlorophyll concentration there was normally less absorption by nonpigmented particles in the spring, which suggests these particulates accumulate during the growing season. In Figure 4a only 55% of the variability of $a_{n(443)}$ with chlorophyll concentration are explained by our data ($n = 175$), whereas *Bricaud et al.* [1998] reported an $r^2 = 0.73$ for $n = 1174$. At lower biomass levels estimates of nonpigmented materials have a higher signal-to-noise ratios with any technique. For chemical extractions sources of variability include changes in particle distributions due to resuspension and/or aggregation, measurement through a different region of the filter, etc. The relative abundance of nonpigmented materials at high latitude is more variable than predicted for lower latitudes by *Bricaud et al.* [1998] and has a larger background level which increases at a much slower rate. Hence during blooms nonpigmented particles play a much smaller role in determining the optical properties of high-latitude waters and blooms with elevated biomass (1–10 mg chlorophyll m^{-3}) are common in brief polar growing seasons.

[28] There have been suggestions that profiles of particulate absorption reveal patterns of photoacclimation, pigment packaging, and the relative abundance of nonpigmented materials [e.g., see *Mitchell and Holm-Hansen*, 1991; *Cleveland*, 1995 and references therein]. *Cleveland* [1995] presented pigment-specific phytoplankton absorption ($\sim a_a^*$) as a function of optical depth from a subpolar fiord which showed that a_a^* generally decreased with depth, but did not identify individual profiles. Obvious trends were difficult to discern. In the Labrador Sea where there is often relatively weak stratification, the lack of vertical patterns is not surprising. In the case of nonpigmented materials there is also sufficient variability that vertical trends are difficult to assess. Nonpigmented materials obviously do not covary closely with chlorophyll (i.e., $r^2 = 0.55$ in Figure 4a). Caution should be used when employing the magnitudes and shapes of absorption spectra to identify photoacclimation status and compositional differences in natural populations unless their variability is well characterized. *Mitchell* [1990] estimated an accuracy of better than ±15% for replicate measurements of particulate absorption by lab cultures; natural assemblages with autotrophs, heterotrophs, and nonliving materials might be expected to be more variable.

[29] There are no large compilations summarizing the absorption properties of soluble materials in the marine environment with broad geographic coverage similar to those of *Bricaud et al.* [1998] for particulate fractions. *Bricaud et al.* [1981] considered a range of environments, but presented only 105 total observations. *Kirk* [1994] considered the subject in general for fresh and marine systems and tabulated estimates for soluble absorption at 440 nm. Off the east coast of the United States environmental conditions ranging from estuarine waters to oligotrophic waters have been characterized by *DeGrandpre et al.* [1996 and references cited therein] and others. The relationship between chlorophyll concentration and soluble absorption at 443 nm (a_{s443}) in the Labrador Sea shown in Figure 4c explains only 2% of the variability in the euphotic zone. Others have noted considerable scatter in similar relationships [*Bricaud et al.*, 1981; *DeGrandpre et al.*, 1996; *Nelson et al.*, 1998]. Figure 5b emphasizes that there is marked variability in the ratio of soluble to total particulate absorption at 443 nm versus chlorophyll concentration, especially at low biomass. Hence their relative influence is extremely variable.

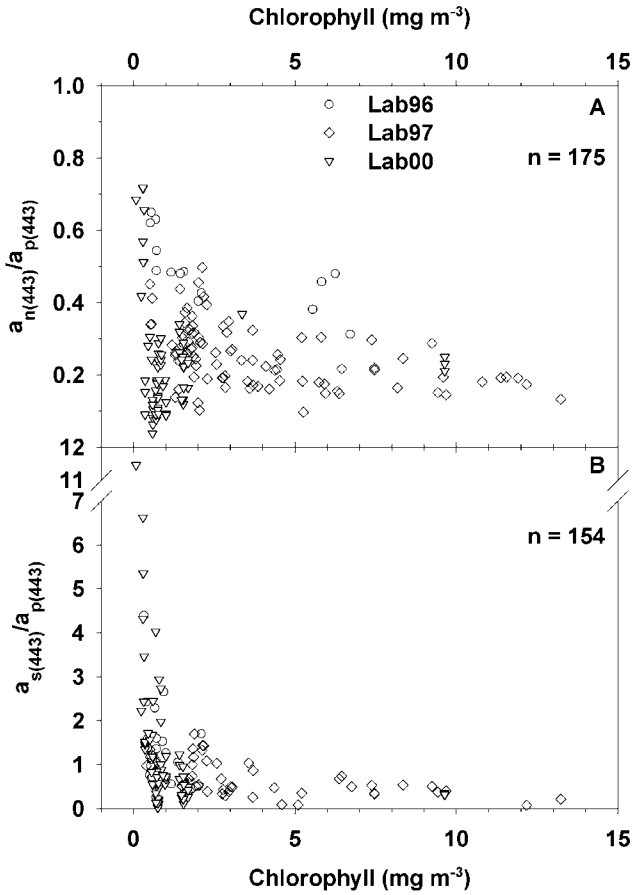

Figure 5. Ratios of (a) nonpigmented and (b) soluble to total particulate absorption at 443 nm versus chlorophyll concentration are shown for 1996 (circles), 1997 (diamonds), and 2000 (inverted triangles).

[30] The sources and sinks for CDOM are rarely evaluated. *Carder et al.* [1989] suggested that CDOM concentrations are related to ecosystem productivity. However, there is considerable regional and seasonal variability, which reflects a snapshot of nonsteady state dynamics between production and destruction of CDOM by biologi-

cal, chemical, and physical processes [e.g., *DeGrandpre et al.*, 1996; *Nelson et al.*, 1998]. Our soluble absorption values at 400 and 443 nm average 0.098 and 0.058 m^{-1}, respectively (Figure 2d). The mean value of S, the logarithmic slope of $a_s(\lambda)$ versus wavelength, for our study was 0.013 nm^{-1} with a standard deviation of 0.002 nm^{-1}. *Kirk* [1994] suggests that typical seawater values for S range from 0.010 to 0.020 nm^{-1} with mean values between 0.012 and 0.015 nm^{-1}. Values >0.020 nm^{-1} may be common in oligotrophic systems [*DeGrandpre et al.*, 1996; *Nelson et al.*, 1998]. The lack of strong covariance of CDOM and chlorophyll reduces the reliability of chlorophyll retrievals and introduces nonsystematic errors for blue-green band ratio algorithms. Errors up to 100–400% have been estimated for band-ratio algorithms in systems with an even broader range of conditions [*Carder et al.*, 1989; *DeGrandpre et al.*, 1996 and references cited therein].

3.4. Modeled Reflectance Spectra

[31] Observed and modeled reflectance spectra are compared in Figure 6. Measured reflectance spectra for 13 wave bands were averaged over bins with chlorophyll concentration ranges of <0.3, >0.3–1, >1–3, >3–10, and >10 mg chlorophyll m^{-3}. With constant conditions, as specified above, simulations were run for mean chlorophyll concentrations corresponding to each bin. Chlorophyll-specific absorption coefficients for phytoplankton (Figure 2c) and nonpigmented (not shown) particulates varied with chlorophyll concentration (Figures 4a and 4b). However, CDOM was held constant at its mean mass-specific concentration (Figure 2d), because it did not covary with chlorophyll concentration (Figure 4c). Variable backscattering to scattering fractions representative of chlorophyll concentration is the key in scaling the magnitude of reflectance signatures [*Ulloa et al.*, 1994; *Mobley et al.*, 2002]. The modeled spectra were generally within the dispersion (±one standard deviation) observed around the mean spectra. This correspondence was used as a subjective measure of model performance, confirming spectral shapes and magnitudes. Reflectance was initially underestimated in the blue but overestimated in the green and red. Agreement was improved considerably by simply increasing the spectral dependency of the scattering, as described above. This serves to emphasize increased scattering at shorter wavelengths by smaller particles. Further model customization might improve the correspondence even further, however, that is beyond the scope of the present effort.

[32] Combining observations for taxonomically diverse phytoplankton assemblages may confound interpretations of generalized cases. Previous simulations with an analytical bio-optical model of the Labrador Sea stressed that group-specific differences in the bio-optical properties of high-latitude phytoplankton assemblages should also be incorporated [*Sathyendranath et al.*, 2001]. These bio-optical differences between groups contributed to taxon-specific discrepancies in chlorophyll retrievals. However, taxon-specific discrimination from satellites is currently not routine.

[33] Discrepancies between observed and modeled reflectances suggest that not all optically active materials are fully accounted for or accurately represented in our reconstructions. Laboratory absorption measurements on discrete samples often do not include all constituents and commonly exclude submicron particles between 0.2 μm (filter-passing "soluble" fraction) and 0.7 μm (the nominal pore size of GF/F filters for particle collection). This size fraction may include abundant nonliving and living particulates such as detritus, nonattached bacteria, and colloidal materials [*Sheldon et al.*, 1972; *Sharp*, 1973; *Koike et al.*, 1990; *Ulloa et al.*, 1994]. Viral particles may also be included in soluble materials. The relative abundance of nonpigmented and algal particles changes with chlorophyll concentration (Figure 5) and the former are often relatively more important at low-biomass levels when they would influence reflectance most. In situ reflectance measurements incorporate the influence of all constituents and exceed model results in the blue in most cases (Figure 6), so the missing size fraction of particles, the phase function, or the spectral dependency of scattering are not completely representative.

[34] For mixed natural assemblages of particles it is convenient to use one general phase function, representing an ensemble average. However, nonpigmented particulates presumably scatter quite differently than phytoplankton cells. They tend to be smaller in size than algal cells with a predominance of nonliving detrital particles (organic and inorganic), larger bacterial cells and attached bacteria. Intact and fragmented debris including silica frustules, calcite particles, spines, carapaces, fecal materials, and sediment should also make this fraction more "minerogenic." Thus these small, abundant particles should be more effective at scattering and at shorter wavelengths. Absorption is also generally low for nonpigmented particles, as determined here on GF/F filters (Figure 2). The optical properties of nonpigmented particulates should be better characterized and incorporated explicitly into more rigorous models.

[35] *Dierssen and Smith* [2000] suggested that blue and green reflectances are higher and lower, respectively, for higher-latitude ecosystems. They compared their Antarctic data with the original "global" data set (n = 919) for the SeaWiFS Bio-optical Algorithm Meeting (SeaBAM) used for the SeaWiFS OC2V1 algorithm described by *O'Reilly et al.* [1998]. However, their reflectances were not significantly different in most bands, presumably because of the large variability in their Antarctic data (see Figures 4–6 of *O'Reilly et al.* [1998]). Only reflectances at 555 nm were consistently lower at chlorophyll concentrations >1 mg m^{-3} (see Table 2 of *O'Reilly et al.* [1998]). By contrast, our reflectance spectra were significantly lower [$P > 0.05$, one-tailed t-test with unequal variances, *Sokal and Rohlf*, 1995] than the SeaBAM spectra [n = 919, *O'Reilly et al.*, 1998] for all six visible SeaWiFS bands (412, 443, 490, 510, 555, and 670 nm) in 26 of 30 cases. Differences were not significant for low biomass of <0.3 mg chlorophyll m^{-3} at 670 nm, moderately low biomass from 1.0 to 3.0 mg chlorophyll m^{-3} at 443 and 490 nm, and high biomass with >10 mg chlorophyll m^{-3} at 412 nm. The first and last cases had small sample sizes of three and seven. Our reflectance spectra for the moderately low-biomass bin from 1.0 to 3.0 mg chlorophyll m^{-3} were the most consistently variable case for the blue-green wave bands, which would influence most algorithms considered below.

[36] The reflectance spectra reported by *Dierssen and Smith* [2000, Figure 6b] also had markedly different shapes compared with ours for similar binned biomass ranges (see

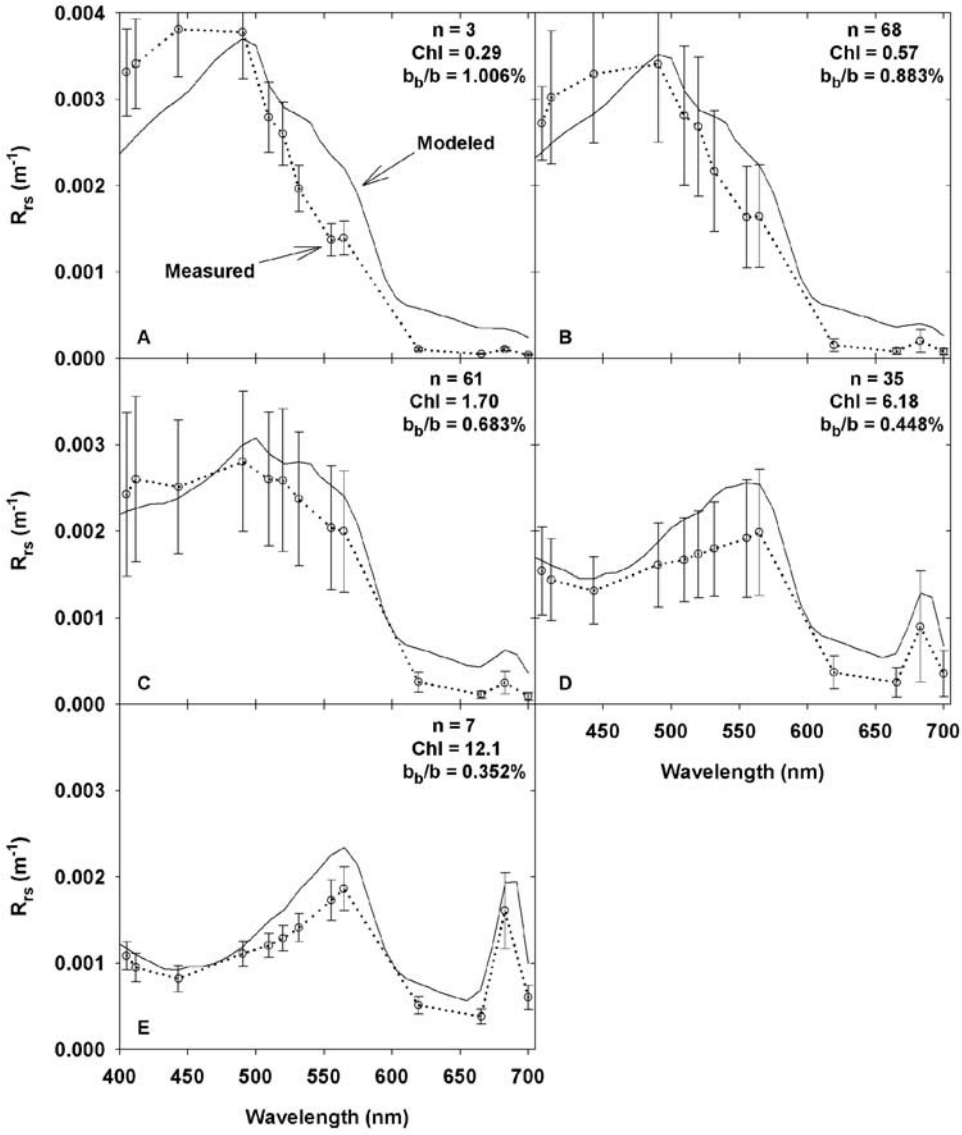

Figure 6. Measured (dotted line) and modeled (solid line) reflectance spectra for biomass bins: (a) <0.3, (b) 0.3–1, (c) 1–3, (d) 3–10, and (e) >10 mg chlorophyll m^{-3}. Mean chlorophyll (Chl) concentrations, the number (n) of observations, and the estimated backscattering to scattering (b_b/b) percentages for each group are presented. Measured spectra are means plus/minus one standard deviation for error bars. See text.

Figure 6). Their spectra all have their highest peaks at 412 nm except for the highest biomass class with >10 mg chlorophyll m^{-3}, perhaps suggesting that CDOM absorption was relatively low in their environment. In contrast, our spectra display peaks from 490 at lower biomass levels to 565 nm at higher ones (see Figure 6). The SeaBAM spectra are similar to ours for biomass >3.0 mg chlorophyll m^{-3}, but also show peaks at 412 nm at lower biomass levels. The SeaBAM data set was dominated by environments with relatively low biomass (Figure 7a), higher light, and lower nutrients [*O'Reilly et al.*, 1998].

[37] *Dierssen and Smith* [2000] postulated that the lower relative abundance of bacteria and viruses in Antarctic waters contributes to the reduced green reflectances. However, we suggest that lower concentrations of small particles would generally reduce reflectance spectra, particularly in the blue (Figure 6). *Li and Harrison* [2001] found that ratios of bacterial to phytoplankton biomass in surface waters of the Labrador Sea (i.e., their Atlantic Arctic and Boreal Polar provinces) were at least 3–5 lower than other oceanic regions in the North Atlantic; similarly picophytoplankton were at least 4–5 times less abundant relative to total phytoplankton biomass. Viruses may also be less abundant. The lower relative abundance of these small biogenic particles presumably contributes to the reduction of reflectances throughout the spectrum as we have observed in the Labrador Sea and in the high Arctic [G. F. Cota, unpublished data, 1994–1996, 1998, 2002; *Wang and Cota*, 2003]. To examine backscattering in their Hydrolight simulations *Dierssen and Smith* [2000, also personal communication] utilized Petzold and Henyey-Greenstein (with g = 0.975) phase functions for all chlorophyll concentration classes.

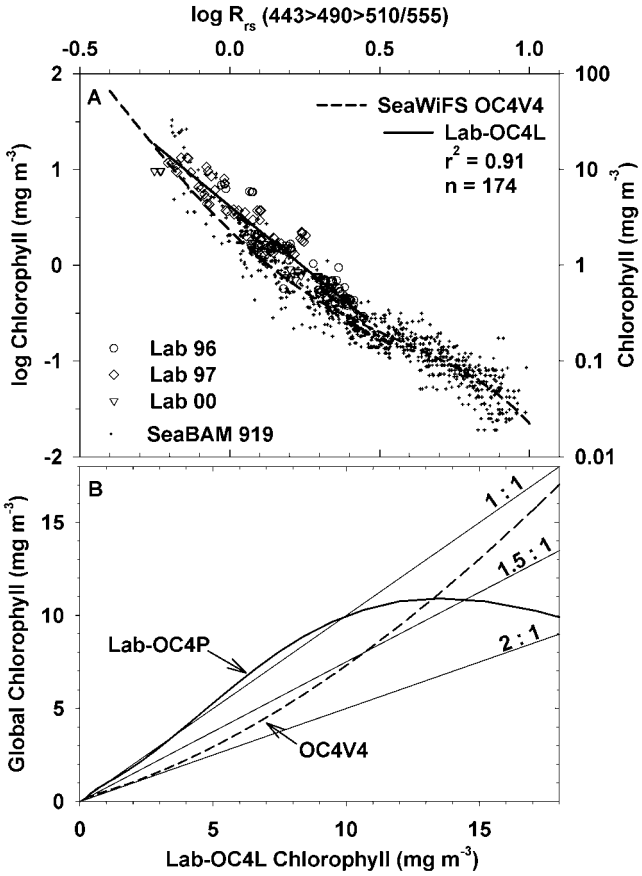

Figure 7. Maximum band-ratio chlorophyll algorithms for the Labrador Sea compared with the current OC4V4 SeaWiFS algorithm. (a) Observed values for 1996 (circles), 1997 (diamonds), and 2000 (inverted triangles) are shown with the original SeaBAM global data set (crosses, $n = 919$). Our linear algorithm Lab-OC4L is shown with SeaWiFS OC4V4. (b) Retrievals from Lab-OC4L are compared with SeaWiFS OC4V4 and our Lab-OC4P algorithms. See text and Table 2 for further details.

These phase functions have respective b_b/b values around 1.83 and 0.53% [*Mobley*, 1994; *Mobley et al.*, 2002], but neither phase function mimicked their data well across the spectrum for all chlorophyll concentrations. Fournier-Forand phase functions with variable b_b/b ratios based on *Ulloa et al.* [1994] proved to be quite successful in our simulated reflectance spectra (Figure 6). We also examined reflectance ratios for 490/555 nm from several phase functions including Petzold, a Henyey-Greenstein with $g = 0.975$, and a Fournier-Forand with a b_b/b of 2%, but found only minor differences for low and high chlorophyll concentrations. Changes in reflectance across the spectrum cancel out to a large degree. The Fournier-Forand phase functions are much more flexible for a range of backscattering to scattering fractions, particle types from biogenic to minerogenic (variable refractive indices), and various particle size distributions [*Mobley*, 1994; *Mobley et al.*, 2002].

3.5. Chlorophyll Algorithms

[38] A four-band ocean color OC4V4 algorithm is the current operational algorithm for global SeaWiFS processing. As described by *O'Reilly et al.* [1998] the OC4 algorithms are maximum band ratios (MBR) for 443 > 490 > 510/555 nm of various functional forms (Table 3). High northern latitude data, primarily from this study and the Canadian Arctic (G. F. Cota, unpublished data, 1994–1996, 1998), now comprise ~11% ($n = 307$) of the most recent global data compilation [$n = 2804$, *O'Reilly et al.*, 2000]. We show the OC2V1 data and OC4V4 algorithm versus our regional data and a linear OC4L algorithm tuned for the Labrador Sea in Figure 7a. The geometric mean for the Labrador Sea of 1.48 mg chlorophyll m^{-3} is much higher than the 0.27 mg chlorophyll m^{-3} of the SeaBAM global data set for OC2V1 [*O'Reilly et al.*, 1998]. Two regional algorithms, the linear, reduced major axis (OC4L) and a fourth-order polynomial (OC4P, not shown), have higher coefficients of determination and lower root mean square errors (RMSE) (Table 3). The OC4V4 global algorithm underpredicts chlorophyll by over 1.5-fold at biomass <10 mg chlorophyll m^{-3}, but can overpredict at very high concentrations (Figure 7b). The linear OC4L regional algorithm is advocated for the most robust chlorophyll retrievals. The OC4P polynomial relationship can be unreliable at high values (Figure 7b).

[39] Additional algorithms for SeaWiFS and OCTS were also compared with our regional bio-optical algorithms tuned with data from the Labrador Sea. These algorithms are described more fully in Table 3. The two-band ocean color OC2 SeaWiFS algorithms (490/555 nm) were based on remote sensing reflectance R_{rs}. The prelaunch version, OC2V1, was developed with a large multiinvestigator data set ($n = 919$) from various locations [*O'Reilly et al.*, 1998]. However, that data set included few high biomass or high-latitude observations. A postlaunch version (OC2V2) was developed with an expanded data set ($n = 1174$) that included even more oligotrophic data and the Antarctic data of *Arrigo et al.* [1998] (J. E. O'Reilly, personal communication, 2000). The OCTS chlorophyll algorithm was a three-band ratio ((520 + 565 nm)/490 nm)) algorithm based on normalized water-leaving radiances L_{wn} [*Kishino et al.*, 1998]. It was developed with a much smaller Japanese data set from North Pacific waters around Japan.

[40] Retrievals from global algorithms can be very misleading, especially at the elevated chlorophyll concentrations common in many blooms and red tides. Large discrepancies (>tenfold) have been noted for red tides off southern California, and there was not consistent agreement across the range of conditions [*Kahru and Mitchell*, 1999]. For high northern latitude waters the at-launch OC2V1 SeaWiFS algorithm overestimated high chlorophyll concentrations of 25 mg m^{-3} about threefold, but underestimated low concentrations. The OC2V2 algorithm underestimated measured chlorophyll concentrations in the Labrador Sea by more than twofold over most of the range. The OCTS chlorophyll algorithm performed reasonably well at low concentrations, but underestimated bloom concentrations. Differences of twofold to tenfold were estimated for CZCS pigment retrievals in the Bering Sea [*Müller-Karger et al.*, 1990].

[41] Group- or species-specific algorithms for phytoplankton are highly attractive because of seasonal succession and potential differences in taxon-specific productivity, export, or carbon cycling [e.g., *Smith et al.*, 1991; *Cota et*

Table 3. Empirical Bio-Optical Algorithms for Chlorophyll (C) Versus Band Ratios (R) Where $R = \log_{10}((L_{wn}520 + L_{wn}565)/L_{wn}490)$ for OCTS and $R = \log_{10}(R_{rs}490/R_{rs}555)$ or $R = \log_{10}((R_{rs}443 > R_{rs}490 > R_{rs}510)/R_{rs}555)$ for SeaWiFS OC2 or OC4 Algorithms, Respectively[a]

Algorithm	Source	Type[b]	Coefficients (a)	Observations	r^2	RMSE
OCTS-C	1	power	−0.5501, 3.497	77	0.95	NR
Lab-OCTS	2	power	−0.4951, 3.5337	174	0.862	0.165
SeaWiFS	3 (OC2V1)	mcp	$a0-a4$[c]	919	0.918	0.172
SeaWiFS	4 (OC2V2)	mcp	$a0-a4$[d]	1174	0.904	0.196
SeaWiFS	5 (OC2V4)	mcp	$a0-a4$[e]	2804	0.883	0.231
SeaWiFS	5 (OC4V4)	4th	$a0-a4$[f]	2804	0.892	0.222
Lab-OC4P	2	4th	$a0-a4$[g]	174	0.914	0.132
Lab-OC4L	2	power	0.6153, −2.576	174	0.908	0.135
Lab-OC4L diatom	2	power	0.7291, −2.258	33	0.778	0.152
Lab-OC4L prymn	2	power	0.5313, −2.400	71	0.947	0.089

[a]SeaWiFS OC2V1 was the at-launch version and the most recent version was OC4V4 (see text). Regional algorithms tuned with our Labrador Sea data are four- (Lab-OC4L and Lab-OC4P, solid and dash-dot lines, Figure 2a) or three-band (Lab-OCTS, solid line, Figure 3a) ratios. Sources: 1, *Kishino et al.* [1998]; 2, this study; 3, *O'Reilly et al.* [1998]; 4, *Maritorena and O'Reilly* [2000]; 5, O'Reilly et al. (personal communication, 2000). RMSE is root mean square error. NR is not reported.

[b]Power is $C = 10^{(a0 + a1R)}$; mcp is modified cubic polynomial, $C = 10^{(a0+a1R+a2R^2+a3R^3)} + a4$; 4th is fourth-order polynomial, $C = 10^{(a0+a1R+a2R^2+a3R^3+a4R^4)}$.

[c]$a0 = 0.3410$; $a1 = -3.0010$; $a2 = 2.8110$; $a3 = -2.0410$; and $a4 = -0.0400$.

[d]$a0 = 0.2974$; $a1 = -2.2429$; $a2 = 0.8358$; $a3 = -0.0077$; and $a4 = -0.0929$.

[e]$a0 = 0.319$; $a1 = -2.336$; $a2 = 0.879$; $a3 = -0.135$; and $a4 = -0.071$.

[f]$a0 = 0.366$; $a1 = -3.067$; $a2 = 1.930$; $a3 = 0.649$; $a4 = -1.532$.

[g]$a0 = 0.627$; $a1 = -3.018$; $a2 = -0.569$; $a3 = 15.58$; and $a4 = -27.86$.

al., 1994]. However, are optical signatures sufficiently distinct to justify taxon-specific satellite algorithms? At present, few such specific algorithms exist, they are derived from small data sets, and most have not been evaluated rigorously.

[42] Figure 8 shows the taxon-specific reflectance ratios for two groups, diatoms (D) and prymnesiophytes (P), and separate algorithms for these taxa. The prymnesiophyte-dominated samples frequently have lower values and overlap markedly with the unidentified (U) assemblages over the range of phytoplankton biomass. On the other hand, the diatom-dominated assemblages tend to have higher reflectance ratios (Figure 8). The OC4L algorithm for the combined data sets is not significantly different [*Sokal and Rohlf*, 1995, $P > 0.05$] from either the prymnesiophyte-dominated assemblages or the unidentified group (not shown). The diatom algorithm is significantly different ($P < 0.05$) from the prymnesiophyte-dominated, unidentified, and combined relationships in Figure 8. Compared with prymnesiophytes the diatom assemblages also have lower specific-absorption coefficients [*Stuart et al.*, 2000; *Sathyendranath et al.*, 2001, this study]. Moreover, at high northern latitudes prymnesiophytes, and *Phaeocystis* in particular, often have higher photosynthetic rates than mixed or diatom-dominated assemblages [*Cota et al.*, 1994; *Stuart et al.*, 2000]. *Arrigo et al.* [1998] also proposed three group- or species-specific algorithms for crytophytes ($n = 6$), diatoms ($n = 31$), and *P. antarctica* ($n = 54$) for the Ross Sea. However, at present, application of these group-specific algorithms seems premature given the degree of overlap in reflectance ratios, the small number of observations, and the restricted ranges of these observations.

[43] There is a large degree of similarity between most algorithms developed at high latitude as shown in Figure 9, where each algorithm is plotted over the range of observations it was developed from without extrapolation. The most striking difference is the D + P algorithm of *Arrigo et al.* [1998] for diatoms plus *Phaeocystis* (prymnesiophytes). Statistical differences between the slopes or intercepts for their algorithm were not reported, but Table 4 and Figure 9 of *Arrigo et al.* [1998] suggests that their diatom, *Phaeocystis*, D + P, and combined algorithms were very similar, perhaps indistinguishable. *Mitchell*'s [1992] algorithms utilized radiance ratios, slightly different spectral bands (488 nm/560 nm), and included chlorophyll plus phaeopigments or "CZCS-pigment." Phaeopigments typically have a very minor influence on these relationships. The remaining polar algorithms in Figure 9 are more similar to one another than the OC2V4 SeaWiFS algorithm [*O'Reilly et al.*, 2000] over most of their ranges. *Mitchell*'s [1992] algorithms for the Arctic and Antarctic, the algorithms of *Arrigo et al.* [1998] for cryptophytes from the Ross Sea, *Dierssen and Smith*'s [2000] algorithm for the Antarctic Peninsula region, and our Labrador Sea algorithm all display similar slopes. The range(s) of data used to develop algorithms can have a

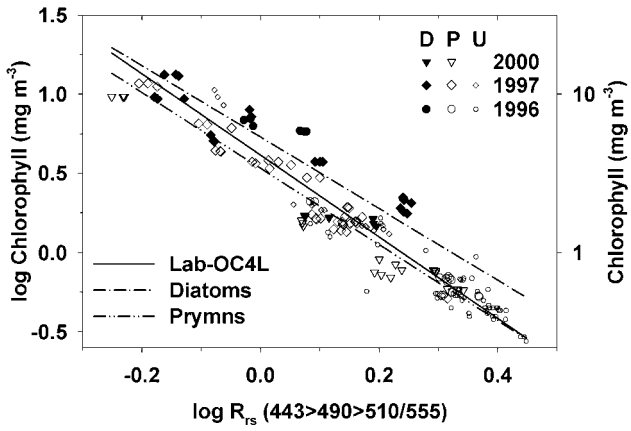

Figure 8. Taxon-specific algorithms for the Labrador Sea are based on pigments diagnostic of diatoms (D, solid symbols), prymnesiophytes (P or Prymnes, open symbols) or unidentified (U, small open symbols) when pigments were not available for each year.

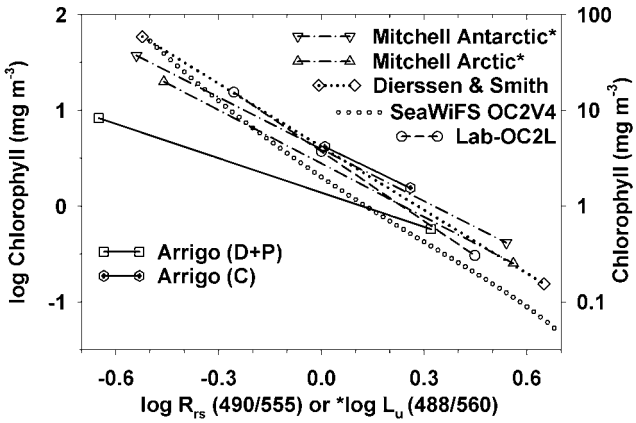

Figure 9. Comparison of high-latitude algorithms. Band-ratio algorithms from this study (Lab-OC2L), the "global" SeaWiFS OC2V4 [*O'Reilly et al.*, 2000], the Antarctic peninsula region [*Dierssen and Smith*, 2000], Ross Sea algorithms from *Arrigo et al.* [1998] for diatoms (D) plus *Phaeocystis* (prymnesiophytes, P) and crytophytes (C), and pigment (chlorophyll plus phaeopigments) algorithms for both polar regions [*Mitchell*, 1992]. Each algorithm is shown for the original range of values.

major influence on the slope of lines and a broad range of environmental conditions is critical to develop robust algorithms. Tuned polar algorithms remain crucial for accurate retrievals of chlorophyll.

4. Conclusions

[44] The bio-optical properties of high-latitude waters are significantly different from lower latitude ecosystems. High-latitude phytoplankton are often larger and are acclimated to low temperature and light regimes. Chlorophyll-specific absorption is lower in polar phytoplankton with more highly packaged pigments. Nonpigmented particle absorption is also relatively low at chlorophyll concentrations above $\sim$1 mg m^{-3} at high latitude. With the observed absorption contributions, a low but variable backscattering fraction, and an increased spectral scattering dependency, modeled reflectance agreed well with observations. Model discrepancies at lower chlorophyll concentrations in the blue and green are attributed to the highly variable influence of nonliving materials (Figure 5) and poorly characterized contributions by small nonpigmented particles, which are weakly absorbing but more minerogenic and more highly scattering. Larger in situ data sets spanning natural variability are needed to develop and validate regional and global relationships. More rigorous modeling efforts should also provide additional insights.

[45] With one serious exception, high-latitude bio-optical algorithms appear to be quite similar [*Arrigo et al.*, 1998; *Mitchell and Holm-Hansen*, 1991; *Mitchell*, 1992; *Dierssen and Smith*, 2000; G. F. Cota, unpublished data, 2002; *Wang and Cota*, 2003]. The current SeaWiFS OC4V4 algorithm underestimates chlorophyll by over 1.5-fold in the Labrador Sea for concentrations <10 mg chlorophyll m^{-3}. Errors of this magnitude would lead to erroneous results in productivity, ecosystem, or biogeochemical models. The OCTS algorithm of *Kishino et al.* [1998] conforms well to our Labrador Sea data except in phytoplankton blooms. Regionally tuned algorithms provide more accurate chlorophyll retrievals.

[46] Several lines of evidence suggest that taxon-specific differences in the bio-optical properties of natural phytoplankton assemblages can be pronounced, especially between diatoms and prymnesiophytes [*Sathyendranath et al.*, 2001, this study]. Although there are taxon-specific differences in absorption and reflectance ratios, it seems premature to rely on their predictive capabilities from space until more data are available and their universality is more firmly established. Further observations and modeling are required to illuminate taxonomic, regional, and seasonal differences.

[47] **Acknowledgments.** This work was supported by NASA's SeaWiFS and SIMBIOS Programs, the Canadian Department of Fisheries and Oceans PERD program, and NASDA's OCTS & GLI Programs. The cooperation of R.A. Clarke, J.R.N. Lazier, and the officers and crew of the CCGC Hudson is greatly appreciated. J.L. Anning, C.S. Clemente, L. Payzant, D.A. Ruble, and J. Wang, provided invaluable assistance. Comments by three anonymous reviewers improved the manuscript.

References

Arrigo, K. R., D. H. Robinson, D. L. Worthen, B. Schieber, and M. P. Lizotte, Bio-optical properties of the southwestern Ross Sea, *J. Geophys. Res.*, *103*, 21,683–21,695, 1998.

Bidigare, R. R., J. L. Iriarte, S.-H. Kang, D. Karentz, M. E. Ondrusek, and G. A. Fryxell, Phytoplankton: Quantitative and qualitative assessments, in *Foundations for Ecological Research West of the Antarctic Peninsula*, *Anarct. Res. Ser.*, vol. 70, edited by R. M. Ross, E. E. Hofmann, and L. B. Quetin, pp. 173–198, AGU, Washington, D. C., 1996.

Bricaud, A., L. Prieur, and A. Morel, Absorption by dissolved organic matter of the sea (yellow substance) in the UV and visible domains, *Limnol. Oceanogr.*, *26*, 43–53, 1981.

Bricaud, A., M. Babin, A. Morel, and H. Claustre, Variability in the chlorophyll-specific absorption coefficients of natural phytoplankton: Analysis and parameterization, *J. Geophys. Res.*, *100*, 13,321–13,332, 1995.

Bricaud, A., A. Morel, M. Babin, K. Allali, and H. Claustre, Variations of light absorption by suspended particles with chlorophyll a concentration in oceanic (case 1) waters: Analysis and implications for bio-optical models, *J. Geophys. Res.*, *103*, 31,033–31,044, 1998.

Brody, E., B. G. Mitchell, O. Holm-Hansen, and M. Vernet, Species-dependent variations of the absorption coefficient in the Gerlache Strait, *Antarct. J. U. S.*, *27*, 160–162, 1992.

Carder, K. L., R. G. Steward, G. R. Harvey, and P. B. Ortner, Marine humic and fulvic acids: Their effects on remote sensing of ocean chlorophyll, *Limnol. Oceanogr.*, *34*, 68–81, 1989.

Cleveland, J. S., Regional models for phytoplankton absorption as a function of chlorophyll *a* concentration, *J. Geophys. Res.*, *100*, 13,333–13,344, 1995.

Cota, G. F., W. O. Smith Jr., and B. G. Mitchell, Photosynthesis of *Phaeocystis* in the Greenland Sea, *Limnol. Oceanogr.*, *39*, 948–953, 1994.

DeGrandpre, M. D., A. Vodacek, R. K. Nelson, E. J. Bruce, and N. V. Blough, Seasonal seawater optical properties of the U.S. Middle Atlantic Bight, *J. Geophys. Res.*, *101*, 22,727–22,736, 1996.

Dierssen, H. M., and R. C. Smith, Bio-optical properties and remote sensing ocean color algorithms for Antarctic Peninsula waters, *J. Geophys. Res.*, *105*, 26,301–26,312, 2000.

Gordon, H. R., and A. Y. Morel, Remote assessment of ocean color for interpretation of satellite visible imagery: A review, in *Lecture Notes on Coastal and Estuarine Studies*, edited by R. T. Barber et al., pp. 1–114, Springer-Verlag, New York, 1983.

Gregg, W. W., and K. L. Carder, A simple spectral solar irradiance model for cloudless maritime atmospheres, *Limnol. Oceanogr.*, *35*, 1657–1675, 1990.

Head, E. J. H., and E. P. W. Horne, Pigment transformation and vertical flux in an area of convergence in the North Atlantic, *Deep Sea Res., Part II*, *40*, 329–346, 1993.

Jeffrey, S. W., and S. W. Wright, Photosynthetic pigments in the Haptophyta, in *The Haptophyte Algae*, edited by J. C. Green and B. S. C. Leadbeater, pp. 111–132, The Syst. Assoc., New York, 1994.

Kahru, M., and B. G. Mitchell, Empirical chlorophyll algorithm and preliminary SeaWiFS validation for the California Current, *Int. J. Remote Sens.*, *20*, 3423–3429, 1999.

Kirk, J. T. O., *Light and Photosynthesis in Aquatic Ecosystems*, pp. 1–509, Cambridge Univ. Press, New York, 1994.

Kishino, M., M. Takahashi, N. Okami, and S. Ichimura, Estimation of the spectral absorption coefficients of phytoplankton in the sea, *Bull. Mar. Sci.*, *37*, 634–642, 1985.

Kishino, M., T. Ishimaru, K. Furuya, T. Oishi, and K. Kawasaki, In-water algorithms for ADEOS/OCTS, *J. Oceanogr.*, *54*, 431–436, 1998.

Koike, I., S. Hara, T. Kazuki, and K. Kogure, Role of sub-micrometre particles in the ocean, *Nature*, *345*, 242–244, 1990.

Li, W. K. W., and W. G. Harrison, Chlorophyll, bacteria, and picophytoplankton in ecological provinces of the North Atlantic, *Deep Sea Res., Part II*, *48*, 2271–2293, 2001.

Loisel, H., and A. Morel, Light scattering and chlorophyll concentration in case 1 waters: A reexamination, *Limnol. Oceanogr.*, *43*, 847–858, 1998.

Maritorena, S., and J. E. O'Reilly, OC2v2: Update on the initial operational SeaWiFS chlorophyll *a* algorithm, *Tech. Memo. 2000-206892*, vol. 11, edited by S. B. Hooker and E. R. Firestone, pp. 3–8, NASA Goddard Space Flight Cent., Greenbelt, Md., 2000.

McClain, C. R., G. Feldman, and W. Esaias, Oceanic biological productivity, in *Atlas of Satellite Observations Related to Global Changes*, edited by R. J. Gurney, J. L. Foster, and C. L. Parkinson, pp. 251–263, Cambridge Univ. Press, New York, 1993.

Mitchell, B. G., Algorithms for determining the absorption coefficient of aquatic particulates using the quantitative filter technique (QFT), in *Ocean Optics X*, pp. 137–148, Int. Soc. for Opt. Eng., Bellingham, Wash., 1990.

Mitchell, B. G., Predictive bio-optical relationships for polar oceans and marginal ice zones, *J. Mar. Syst.*, *3*, 91–105, 1992.

Mitchell, B. G., and O. Holm-Hansen, Bio-optical properties of Antarctic Peninsula waters: Differentiation from temperate ocean models, *Deep Sea Res., Part A*, *38*, 1009–1028, 1991.

Mobley, C. D., *Light and Water: Radiative Transfer in Natural Waters*, 592 pp., Academic, San Diego, Calif., 1994.

Mobley, C. D., L. K. Sundman, and E. Boss, Phase function effects on oceanic light fields, *Appl. Opt.*, *41*, 1035–1050, 2002.

Mueller, J. L., and R. W. Austin, *Ocean Optics Protocols for SeaWiFS Validation*, revision 1, pp. 1–67, NASA, Greenbelt, Md., 1995.

Müller-Karger, F. E., C. R. McClain, R. N. Sambrotto, and G. C. Ray, A comparison of ship and coastal zone color scanner mapped distribution of phytoplankton in the southeastern Bering Sea, *J. Geophys. Res.*, *95*, 11,483–11,499, 1990.

Nelson, N. B., D. A. Siegel, and A. F. Michaels, Seasonal dynamics of colored dissolved material in the Sargasso Sea, *Deep Sea Res., Part I*, *45*, 931–957, 1998.

O'Reilly, J. E., S. Maritorena, B. G. Mitchell, D. A. Siegel, K. L. Carder, S. A. Garver, M. Kahru, and C. McClain, Ocean color chlorophyll algorithms for SeaWiFS, *J. Geophys. Res.*, *103*, 24,937–24,953, 1998.

O'Reilly, J. E., et al., Ocean color chlorophyll *a* algorithms for SeaWiFS, OC2 and OC4: Version 4, *NASA Tech. Memo. 2000-206892*, vol. 11, edited by S. B. Hooker and E. R. Firestone, pp. 9–23, NASA Goddard Space Flight Cent., Greenbelt, Md., 2000.

Parsons, T. R., M. Takahashi, and B. Hargrave, *Biological Oceanographic Processes*, 3rd ed., 323 pp., Pergamon, New York, 1984.

Pope, R. M., and E. S. Fry, Absorption spectrum (380–700 nm) of pure water, part II, Integrating cavity measurements, *Appl. Opt.*, *36*, 8710–8723, 1997.

Sathyendranath, S., G. Cota, V. Stuart, H. Maass, and T. Platt, Remote sensing of phytoplankton pigments: A comparison of empirical and theoretical approaches, *Int. J. Remote Sens.*, *22*, 249–273, 2001.

Sharp, J. H., Size classes of organic carbon in seawater, *Limnol. Oceanogr.*, *18*, 441–447, 1973.

Sheldon, R. W., A. Prakash, and W. H. Sutcliffe Jr., The size distribution of particles in the ocean, *Limnol. Oceanogr.*, *17*, 327–340, 1972.

Smith, R. C., and K. S. Baker, Optical properties of the clearest natural waters (200–800 nm), *Appl. Opt.*, *20*, 177–184, 1981.

Smith, W. O., Jr., L. A. Codispoti, D. M. Nelson, T. Manley, E. J. Buskey, H. J. Niebauer, and G. F. Cota, Importance of *Phaeocystis* blooms in the high-latitude ocean carbon cycle, *Nature*, *352*, 514–516, 1991.

Sokal, R. R., and F. J. Rohlf, *Biometry*, 3rd ed., 887 pp., W.H. Freeman, New York, 1995.

Stauber, J. L., and S. W. Jeffrey, Photosynthetic pigments in fifty-one species of marine diatoms, *J. Phycol.*, *24*, 158–172, 1988.

Steemann Nielsen, E., A survey of recent Danish measurements of the organic productivity in the sea, *J. Cons. Cons. Perm. Int. Explor. Mer.*, *144*, 92–95, 1958.

Stuart, V., S. Sathyendranath, E. J. H. Head, T. Platt, B. Irwin, and H. Maass, Bio-optical characteristics of diatom and prymnesiophyte populations in the Labrador Sea, *Mar. Ecol. Prog. Ser.*, *201*, 91–106, 2000.

Ulloa, O., S. Sathyendranath, and T. Platt, Effect of the particle-size distribution on the backscattering ratio in seawater, *Appl. Opt.*, *33*, 7070–7077, 1994.

Wang, J., and G. F. Cota, Remote sensing reflectance in the Beaufort and Chukchi Seas: Observations and models, *Appl. Opt.*, *42*, 2754–2765, 2003.

G. F. Cota, Center for Coastal Physical Oceanography, Old Dominion University, 768 West 52nd Street, Norfolk, VA 23508, USA. (cota@ccpo.odu.edu)

W. G. Harrison, T. Platt, and V. Stuart, Biological Oceanography, Bedford Institute of Oceanography, Dartmouth, Nova Scotia, Canada, B2Y 4A2. (harrisong@mar.dfo_mpo.gc.ca; tplatt@dal.ca; vstuart@dal.ca)

S. Sathyendranath, Department of Oceanography, Dalhousie University, Halifax, Nova Scotia, Canada, B3H 4J1. (shubha@dal.ca)